Physiological Roles of the Intermediate Conductance, Ca 2 +-activated Potassium Channel Kcnn4

THE JOURNAL OF BIOLOGICAL CHEMISTRY
Vol. 279, No. 46, Issue of November 12, pp. 47681–47687, 2004
Printed in U.S.A.

Physiological Roles of the Intermediate Conductance, Ca^{2+}-activated Potassium Channel Kcnn4*

Received for publication, August 23, 2004, and in revised form, September 1, 2004
Published, JBC Papers in Press, September 3, 2004, DOI 10.1074/jbc.M409627200

Ted Begenisich‡, Tesuji Nakamoto§, Catherine E. Ovitt§, Keith Nehrke¶, Carlo Brugnara‖, Seth L. Alper‡‡§§, and James E. Melvin§¶¶**

*From the Departments of ‡Pharmacology and Physiology and ¶Medicine and the §Center for Oral Biology in the Aab Institute for Biomedical Sciences, University of Rochester Medical Center, Rochester, New York 14642, the ‖Department of Laboratory Medicine, The Children's Hospital, Boston, Massachussetts 02115, and the ‡‡Molecular and Vascular Medicine Unit and Renal Division, Beth Israel Deaconess Medical Center and the Departments of §§Medicine and **Pathology, Harvard Medical School, Boston, Massachussetts 02215*

Three broad classes of Ca^{2+}-activated potassium channels are defined by their respective single channel conductances, *i.e.* the small, intermediate, and large conductance channels, often termed the SK, IK, and BK channels, respectively. SK channels are likely encoded by three genes, *Kcnn1–3*, whereas IK and most BK channels are most likely products of the *Kcnn4* and *Slo* (*Kcnma1*) genes, respectively. IK channels are prominently expressed in cells of the hematopoietic system and in organs involved in salt and fluid transport, including the colon, lung, and salivary glands. IK channels likely underlie the K^+ permeability in red blood cells that is associated with water loss, which is a contributing factor in the pathophysiology of sickle cell disease. IK channels are also involved in the activation of T lymphocytes. The fluid-secreting acinar cells of the parotid gland express both IK and BK channels, raising questions about their particular respective roles. To test the physiological roles of channels encoded by the *Kcnn4* gene, we constructed a mouse deficient in its expression. *Kcnn4* null mice were of normal appearance and fertility, their parotid acinar cells expressed no IK channels, and their red blood cells lost K^+ permeability. The volume regulation of T lymphocytes and erythrocytes was severely impaired in *Kcnn4* null mice but was normal in parotid acinar cells. Despite the loss of IK channels, activated fluid secretion from parotid glands was normal. These results confirm that IK channels in red blood cells, T lymphocytes, and parotid acinar cells are indeed encoded by the *Kcnn4* gene. The role of these channels in water movement and the subsequent volume changes in red blood cells and T lymphocytes is also confirmed. Surprisingly, Kcnn4 channels appear to play no required role in fluid secretion and regulatory volume decrease in the parotid gland.

It has become clear that multiple types of Ca^{2+}-activated potassium channels underlie a wide range of distinct physiological processes. Physiological and pharmacological analyses have subdivided Ca^{2+}-activated potassium channels into three groups, *i.e.* the small, intermediate, and large conductance channels, often termed SK,[1] IK, and BK channels, respectively. IK channels, as their designation implies, have a single channel conductance intermediate between the SK and BK channels. These three functional groups have rather distinct pharmacological profiles, and SK, IK, and BK channels can be specifically blocked by apamin, clotrimazole, and paxilline, respectively. SK and IK channels are encoded by four genes of the *KCNN* gene family. The three SK channels, KCNN1–3, share ~70–75% amino acid identity. The IK channel KCNN4 is encoded by a protein sharing only ~40% amino acid identity with each of the three SK channels, KCNN1–3.

KCNN4 channels are prominently expressed in cells of the hematopoietic system and in organs involved in salt and fluid transport, including the colon, lung, and salivary glands (1–5). Heterologous expression of KCNN4 produces K^+-selective, Ca^{+2}-activated channels without time or voltage dependence (1–4, 6). The expressed channels are sensitive to clotrimazole, but the reported affinity appears to depend on the expression system used (compare, for example, Refs. 2 and 3). These channels are also sensitive to inhibition by charybdotoxin, stichodactyla toxin, and maurotoxin but are insensitive to the SK blocker apamin and the BK blocker iberiotoxin.

Red blood cells have a high but latent passive permeability to K^+ ions that is mediated by what is often called the Gardos channel (7). This channel has all the properties of, and is likely encoded by, the *KCNN4* gene (4, 8). Increased water loss from red blood cells secondary to increased K^+ permeability is a contributing factor in the pathophysiology of sickle cell disease. The resulting increase in the intracellular concentration of hemoglobin S leads to a shortened delay time for the polymerization of deoxyhemoglobin S. Thus, blocking erythrocyte K^+ permeability and the consequent dehydration is under evaluation as a potential therapy for sickle cell disease. Indeed, blocking the red blood cell IK channel with clotrimazole prevents erythrocyte dehydration in patients with sickle cell disease (9, 10) and in a mouse model of sickle cell disease (11, 12).

The *KCNN4* gene also likely encodes the Ca^{2+}-activated, intermediate conductance K^+ channel expressed in T lymphocytes (3). This channel is expressed at low levels in human resting T cells and is strongly up-regulated during activation by mitogens (13). The role of the IK channel in lymphocytes appears to be the maintenance of a hyperpolarized membrane

* This work was supported by National Institutes of Health Grants DE08921, DE09692, and DE013539 (to J. E. M., T. B., T. N., and C. E. O.), DK57662 and DK61051 (to S. L. A.), DK34854 (to the Harvard Digestive Diseases Center), and HL73112 and DK50422 (to C. B.). The costs of publication of this article were defrayed in part by the payment of page charges. This article must therefore be hereby marked "*advertisement*" in accordance with 18 U.S.C. Section 1734 solely to indicate this fact.

¶¶ To whom correspondence should be addressed: Center for Oral Biology, Medical Center Box 611, 601 Elmwood Ave., Rochester NY 14642. Tel.: 585-275-3444; Fax: 585-276-0190; E-mail: james_melvin@urmc.rochester.edu.

[1] The abbreviations used are: SK, small potassium conductance; IK, intermediate potassium conductance; BK, large potassium conductance; MOPS, 4-morpholinepropanesulfonic acid; NS, normal saline; RVD, regulatory volume decrease.

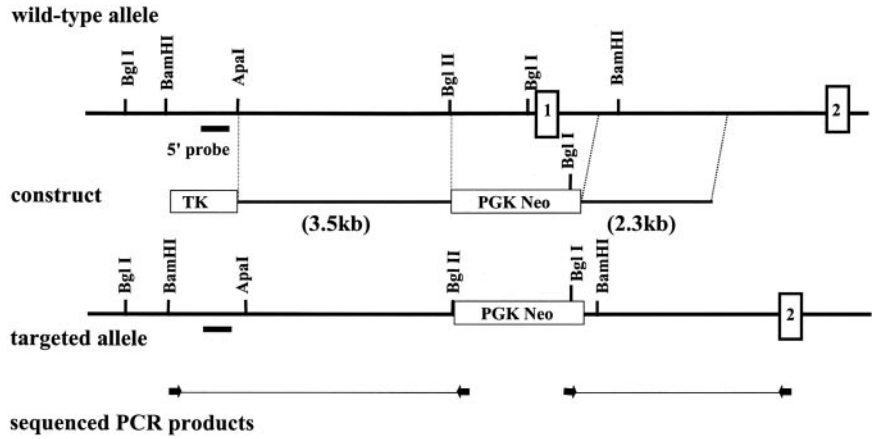

FIG. 1. ***Kcnn4* gene targeting.** Schematic diagram of the 5′-end of the *Kcnn4* gene locus (*top*), the targeting construct (*middle*), and the targeted allele (*bottom*). Only exons 1 and 2 are shown. A region of 1.7 kb surrounding and including the first exon was replaced by the phosphoglycerate kinase-*Neo* (*PGK-Neo*) cassette, and the gene for thymidine kinase (*TK*) was included upstream for negative selection. The lengths of homology for the 5′- and 3′-arms are 3.5 and 2.3 kb, respectively. The position of the 5′-probe used for Southern blot analysis is indicated. In addition, at *bottom* are shown the genomic PCR products that were amplified and sequenced to confirm the integrity of recombination at both ends.

potential, thus facilitating and maintaining the intracellular Ca^{2+} levels required for mitogen activation (14, 15). The cell shrinkage that correlates with the initiation of apoptosis in T lymphocytes is specifically blocked by clotrimazole, suggesting that IK1 may also be involved in early events associated with apoptosis in this cell type (16).

In most fluid-secreting exocrine epithelia, the acinar cell cytoplasmic Cl^- concentration is maintained above electrochemical equilibrium by the Na-K-2Cl transporter. The exit of Cl^- into the lumen is balanced by the movement of Na^+ ions through the interstitial tight junctions into the lumen. This elevated salt concentration draws water into the lumen and, after modification by the duct cells, leads to a secreted fluid rich in NaCl.

To maintain fluid secretion, the Cl^- efflux into the lumen must be sustained. In the absence of any other active channels, the acinar cell membrane potential would approach the Cl^- equilibrium potential and net Cl^- movement would cease. Both exocrine and other fluid-secreting epithelia often express K^+ channels whose activity can facilitate Cl^- efflux by maintaining a hyperpolarized membrane voltage. Rodent (and other) salivary glands express two types of Ca^{2+}-activated potassium channels, a BK channel and an IK channel (17–22). These BK and IK channels have biophysical and pharmacological properties consistent with those expected of channels encoded by the *Slo* (*Kcnma1*) and *Kcnn4* genes, respectively (6, 22). Both channels are activated by the increase in intracellular Ca^{2+} produced by muscarinic agonists, but the evidence suggests that fluid secretion may be independent of BK channel activity (17, 20, 23), leaving IK channels to play this role.

Kcnn4 is believed to play important roles in the volume regulation of circulating blood cells such as lymphocytes (15) and erythrocytes (10), which traverse the hyperosmotic environment of the renal medulla. In lymphocytes, Kcnn4-mediated hyperpolarization promotes sustained elevation of cytoplasmic Ca^{2+} levels, which permits the modulation of gene expression via the regulated nuclear translocation of transcription factors. In sickle disease erythrocytes the hyperactivation of Kcnn4 contributes, via cell shrinkage and the increased concentration of hemoglobin S, to the pathological acceleration of deoxyhemoglobin S polymerization. This, in turn, accelerates cell sickling and increases the likelihood of vaso-occlusion.

To test for the physiological roles of IK channels, we have inactivated the *Kcnn4* gene in mouse by homologous recombination. Homozygous mice carrying this knock-out appeared grossly normal and were fertile. We found the expected loss of functional IK1 channels in T lymphocytes, erythrocytes, and parotid acinar cells, confirming the genetic basis for this channel type. Disrupting the expression of the *Kcnn4* gene impaired the volume regulation of T lymphocytes and erythrocytes but not that of parotid acinar cells. Despite the loss of IK channels, activated fluid secretion from the parotid glands was normal.

EXPERIMENTAL PROCEDURES

Gene Targeting and Molecular Techniques

Gene Targeting—The targeting vector for homologous recombination was constructed using the pKO Scrambler V1901 vector (Lexicon Genetics), which contains the *Neo* gene driven by the phosphoglycerate kinase promoter. A mouse *IK1* genomic clone was isolated from an SVJ129 lambda library using a probe specific to exons 1 and 2 and standard screening techniques. The 5′-arm was created as a BglII-tagged fragment by low round PCR amplification from the excised IK1 genomic insert. The 3′-arm was isolated directly from the genomic clone as a BglII (genomic)/NotI(vector) fragment. All clones were sequenced for verification. The 5′-arm was inserted into the pKO Scrambler V1901 vector's BglII site, and the 3′-arm was inserted into the vector's BamHI and NotI sites. The phosphoglycerate kinase-*Neo* cassette lies between the arms in the opposite orientation (Fig. 1). The targeting vector was linearized with NotI and electroporated into CJ7 embryonic stem cells. Southern blot analysis identified several positive clones, one of which was expanded and injected into blastocysts. Chimeric male mice were bred to C57Bl/6J female mice. Breeder pairs from the resulting heterozygous offspring were used to generate wild-type, heterozygous, and homozygous null littermates for all of the subsequent experiments. All experimental protocols were approved by the Animal Resources Committee of the University of Rochester.

Genotyping and Southern Analysis—DNA was isolated from tail clips using standard procedures. Initial characterization of the targeting event was performed on Southern blots with hybridization to the 250-bp 5′-outside probe (Fig. 1). In addition, PCR products were obtained using the Triple Master PCR System (Eppendorf), which span both ends of the recombination (indicated in Fig. 1). Sequencing of these products across the recombination sites confirmed that the targeting vector has integrated at the expected site in the mouse IK1 locus (data not shown). Routine genotyping of mice for functional assays was done using standard PCR protocols.

Northern Blots—Parotid salivary glands were dissected from adult wild-type, heterozygous, and homozygous knockout mice. CD4+ T cells were isolated using the protocol described below under the section entitled "CD4+ T Lymphocyte Methods." Either the RNeasy kit (Qiagen) or Trizol reagent (Invitrogen) was used to isolate total RNA from all tissues. mRNA was prepared using oligo(dT) mini columns (Qiagen). 15 μg of total RNA or 5 μg of mRNA were separated on a 1% agarose/2.2 M formaldehyde gel and blotted. The blots were hybridized with a full-length probe for the Kcnn4 coding sequence, the total RNA blot in Church buffer (0.5 M $NaPO_4$, pH 7.2, 7% SDS, and 1 mM EDTA) at 65 °C, and the mRNA blot in ExpressHyb reagent (Clontech) per the manufacturer's instruction. Marker sizes are based on 18 and 28 S bands or an RNA ladder (Invitrogen).

Parotid Gland Methods

Acinar Cell Preparation—Acinar cells were obtained from age- and sex-matched littermates by enzyme digestion as described in our previous reports (6, 24), with some modifications. In brief, mice were anesthetized by exposure to CO_2 gas and killed by exsanguination via cardiac puncture. The parotid glands were dispersed in a digestion solution composed of Eagle's minimum essential medium (Biofluid),

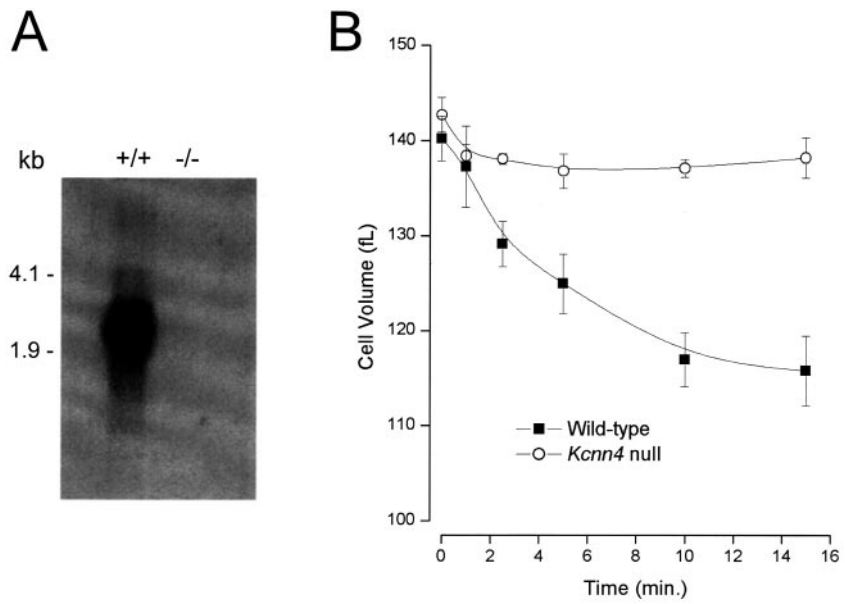

FIG. 2. **Northern analysis and cell volume measurements of CD4+ T lymphocytes.** *A*, Northern analysis of total RNA (15 μg) from CD4+ T lymphocytes of wild-type (+/+) and *Kcnn4* null (−/−) adult mice. The blot was hybridized to a full-length probe for the mouse IK1 coding sequence. *B*, cell volumes from mouse CD4+ T lymphocytes recorded using a Coulter counter and Channelyzer. Cell shrinkage was induced by the addition of the Ca^{2+} mobilizing agent ionomycin (5 μM) to CD4+ T lymphocytes from wild-type mice (■; n = 6) or lymphocytes from *Kcnn4* null animals (○; n = 6). Cell volume is expressed as mean ± S.E. limits in units of femtoliters (*fL*) per cell.

0.17 mg/ml Liberase RI enzyme (Roche Applied Science), 1% bovine serum albumin, and 2 mM L-glutamine at 35–37 °C. Parotid tissue was minced with fine scissors in digestion buffer and incubated for 20 min. Cells were dispersed by pipetting every 10 min followed by rinsing with basal medium (Eagle) with 1% bovine serum albumin. To obtain single cells, the minced tissue was initially incubated in digestion solution containing 0.1% trypsin and 5 mM EDTA for 5 min and then further digested as described above in the presence of a 0.2% trypsin inhibitor.

Cell Volume Measurement—Isolated acinar cells were incubated with 2 μM calcein-acetoxymethyl ester in basal medium (Eagle) with 1% BSA for 20 min and then washed twice. Cells were attached to a coverslip on the base of a 500-μl chamber and perfused with bicarbonate-free physiologic salt solution containing 105 mM NaCl, 25 mM sodium gluconate, 5.4 mM KCl, 2.2 mM $CaCl_2$, 0.8 mM $MgSO_4$, 0.33 mM NaH_2PO_4, 0.4 mM KH_2PO_4, 10 mM glucose, and 20 mM Hepes (pH 7.4, with NaOH) at room temperature (20–22 °C). The hypotonic shock solution was made by adding a 30% volume of distilled water. The perfusion chamber was mounted on an inverted microscope (Nikon Diaphot 200) interfaced with a fluorescence imaging system (TILL) and perfused at 3 ml/min. Fluorescence images were collected at 10-s intervals using 20-msec exposures at 490-nm excitation and 530-nm emission wavelengths. Cell volume changes were expressed as 1 per normalized fluorescence as reported previously (24). Quantitative estimates of the rates of cell volume change were made using the early linear phase of volume recovery. Channel inhibitors were introduced 2 min prior to the hypotonic shock.

In Vivo Saliva Collection—Mice were anesthetized by intraperitoneal injection of chloral hydrate (500 mg/kg) prior to isolating the ducts from the left and right parotid glands with the aid of a dissecting microscope. The trachea was exposed and incised to ensure a patent airway during the experiment. Body temperature was maintained at 37 °C using a regulated blanket (Harvard Apparatus). The cut ends of the ducts were inserted into individual calibrated glass capillary tubes (VWR Scientific). Secretion was stimulated by intraperitoneal injection of secretagogues. Saliva was collected for 30 min and stored at −86 °C. At the end of the saliva collection period, blood was collected by cardiac puncture into heparinized syringes, and mice were euthanized by exposure to CO_2 gas. Parotid glands were removed and carefully trimmed of connective tissue under a dissecting microscope.

Salivary flow rate was expressed as 1 μl per 100 mg of gland weight. Sodium and potassium concentrations were measured by atomic absorption (PerkinElmer Life Sciences 3030 spectrophotometer). Chloride activity was measured using an Orion Research expandable ion analyzer 940. Sample osmolality was obtained with a Wescor 5500 vapor pressure osmometer. Protein concentration was estimated by a BCA protein assay reagent kit (Pierce).

Electrophysiology—Whole-cell patch clamp recordings were made at room temperature (20–22 °C) with an Axopatch 1-D amplifier (Axon Instruments, Foster City, CA). Data acquisition was performed using a 12-bit analog/digital converter controlled by a personal computer. We used an internal solution that consisted of 135 mM potassium glutamate, 10 mM HEPES (pH 7.2), 5 mM EGTA, and 3 mM $CaCl_2$, which established a free Ca^{2+} concentration of 250 nM (25) (see also www.stanford.edu/~cpatton/maxc.html). The external solution consisted of 135 mM sodium glutamate, 5 mM potassium glutamate, 2 mM $CaCl_2$, 2 mM $MgCl_2$, and 10 mM HEPES, pH 7.2.

CD4+ T Lymphocyte Methods

CD4+ T lymphocytes were isolated using a $CD4^+$ Cell Isolation kit (Mitenyi Biotec; Auburn, CA). Briefly, mice were killed by exposure to CO_2. Lymph nodes (including inguinal, brachial, axillary, superficial cervical, and mesenteric nodes) were removed, placed in RPMI medium (Invitrogen) containing 10% fetal bovine serum, 1% Pen/Strep, 1% L-glutamine, and 0.0002% 2-mercaptoethanol) and then gently forced through a 70-μm nylon cell strainer (Falcon 352350; BD Biosciences). The resulting cell suspension was transferred through a 40-μm nylon cell strainer (Falcon 352340; BD Biosciences) and then centrifuged at 4 °C and 1200 rpm (~250 g) for 5 min. Cells were resuspended in degassed PBS buffer (with 1% fetal bovine serum and 2 mM EDTA) containing a biotin-antibody mixture and incubated for 10 min at 4 °C. Anti-biotin microbeads were added for an additional 15 min at 4 °C, the suspension was rinsed, and then CD4+ T lymphocytes were isolated on MACS separation columns (Mitenyi Biotec; Auburn, CA). Cells were kept on ice in the RPMI solution until use. Cell volume was determined using a Coulter counter and Channelyzer (Beckman Coulter Electronics Inc.). Cell volume determinations were performed using software from Coulter Electronics Inc. (AccuComp version 4.1A) and expressed in femtoliters per cell.

Erythrocyte Methods

$^{86}Rb^+$ Influx—$^{86}Rb^+$ influx into mouse erythrocytes was measured using a variation of previously described methods (11, 26). Heparinized blood was washed five times in 10 volumes of choline wash solution (172 mM choline chloride, 1 mM $MgCl_2$, 10 mM Tris-MOPS, pH 7.4, at 4 °C) and then washed once in normal saline (NS) (165 mM NaCl, 2 mM KCl, 0.15 mM $MgCl_2$, 10 mM Tris-MOPS, pH 7.4) and resuspended at room temperature with a hematocrit of 3% in flux medium (NS supplemented with 50 μM $CaCl_2$, 1 mM ouabain, 100 μM bumetanide, and 10 μCi/ml $^{86}Rb^+$) in the absence or presence of 10 μM clotrimazole. The influx assay was initiated by the addition of 5 μM A23187 (from 1 mM ethanol stock) or vehicle alone to the erythrocyte suspension. Triplicate 100-μl aliquots of vortexed cell suspension were withdrawn at influx times of 2 and 5 min. These aliquots were immediately added to precooled 1.5-ml tubes containing 0.8 ml of NS plus 5 mM EGTA layered over 0.3 ml of phthalate. Samples were centrifuged at 14,000 rpm for 15 s. After removal of the aqueous upper layers and part of the oil layer, the tube tips were cut off and counted in a γ-counter. Influx was calculated from the linear slope derived from the mean values at 2 and 5 min and expressed in units of mmol K(Rb)/10^{13} cells × h^{-1}. KCNN4-mediated flux was expressed as the clotrimazole-sensitive component of $^{86}Rb^+$ influx in the presence of A23187.

Osmotic Fragility—Mouse erythrocytes washed three times in NS

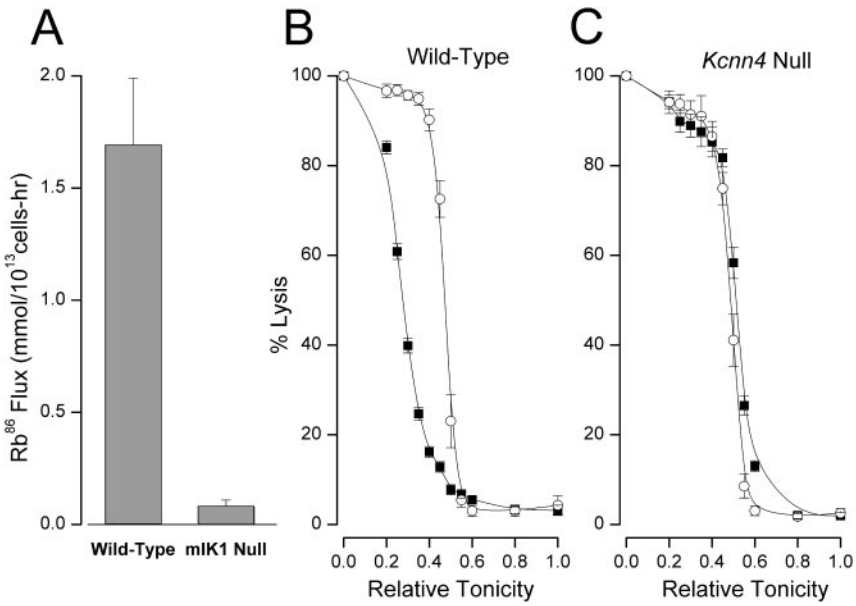

FIG. 3. **Indices of IK1 activity in red cells.** *A*, A23187-stimulated, clotrimazole-sensitive ^{86}Rb influx into red cells from wild-type and *Kcnn4* null mice. Values are means ± S.E. from wild-type (n = 20) and *Kcnn4* null (n = 21) mice. *B*, percentage of lysis of red blood cells at the indicated relative tonicity from wild-type mice in the absence (○) and presence (■) of the Ca^{2+} ionophore A23187. *C*, osmotic lysis of red cells from *Kcnn4* null mice in the absence (○) and presence (■) of A23187. *Lines* connecting the data points have no theoretical meaning.

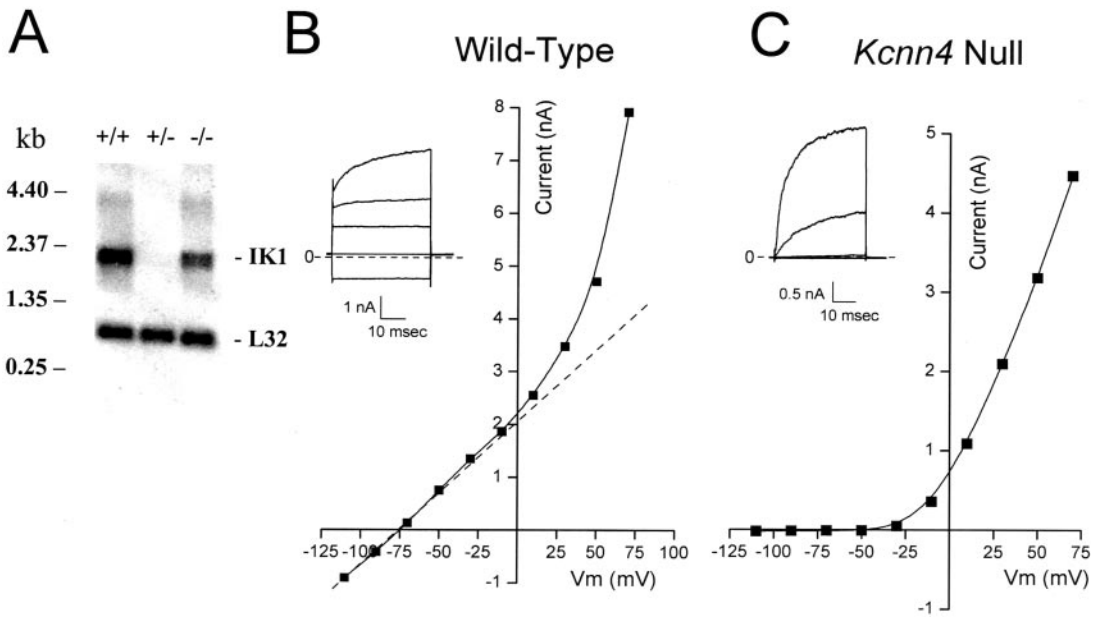

FIG. 4. **Northern analysis and electrophysiology of parotid acinar cells.** *A*, Northern analysis of mRNA (5 μg) from parotid glands of wild-type (+/+), heterozygous (+/−), and *Kcnn4* null (−/−) adult mice. The blot was hybridized to a full-length probe for the mouse IK1 coding sequence. Subsequent hybridization with a mouse ribosomal mRNA L32 probe confirmed RNA loading. *B*, raw currents and current-voltage relation from a wild-type mouse parotid gland cell recorded in whole-cell mode. The *inset* depicts currents in response to 40-msec voltage pulses to −110, −30, +10, and +50 mV from a holding potential of −70 mV. In the main figure, currents are measured at the end of pulses to the indicated membrane voltages. The *dashed line* represents the linear (mouse IK1) current component; the data values above this line represent the non-linear, time-dependent (Slo channel) component. *C*, raw whole-cell currents and current-voltage relation from a parotid gland cell of *Kcnn4* null mouse. The format is the same as for *panel B*.

were resuspended to 5% hematocrit in isotonic lysis solution (NS buffered by 10 mM Tris-HEPES, pH 7.5 at 20 °C) in the absence or presence of 5 μM A23187 and then incubated for 30 min at room temperature. Triplicate 10-μl aliquots of cell suspension were transferred to microfuge tubes containing 290-μl lysis solutions of the indicated relative tonicity prepared by proportional mixing of NS buffered by 2 mM Tris-HEPES (relative tonicity of 1) with 2 mM Tris HEPES-buffered water (relative tonicity of 0). After thorough mixing, tubes were centrifuged at 4000 rpm × 5 min, and 250-μl aliquots of each supernatant were removed for measurement of A_{540}. A_{540} values at zero relative tonicity were defined as 100% lysis for normalization.

RESULTS

The mouse *Kcnn4* gene was inactivated by homologous recombination in embryonic stem cells. A targeting vector was constructed with 3.5- and 2.3-kb homologous arms of *Kcnn4* genomic sequence, completely deleting exon 1. Homologous recombinants were identified by Southern blot analysis, and a positively identified recombinant clone was injected into blastocysts. Germline transmission was confirmed through Southern hybridization and PCR analyses of tail samples from the progeny of the chimeric founders (Fig. 1). Mating mice heterozygous for the inactivated allele of *Kcnn4* produced 425 offspring; of these, 103 were homozygous wild-type (+/+), 228 were heterozygous (±), and 94 were homozygous *Kcnn4* null (−/−) animals representing 24, 54, and 22% of the number of births, respectively. This distribution is nearly identical to the normal Mendelian frequency of 25, 50, and 25%. The *Kcnn4*(−/−) mice appeared to develop normally. Homozygous (−/−) mice of both sexes were fertile. Body weights of homozy-

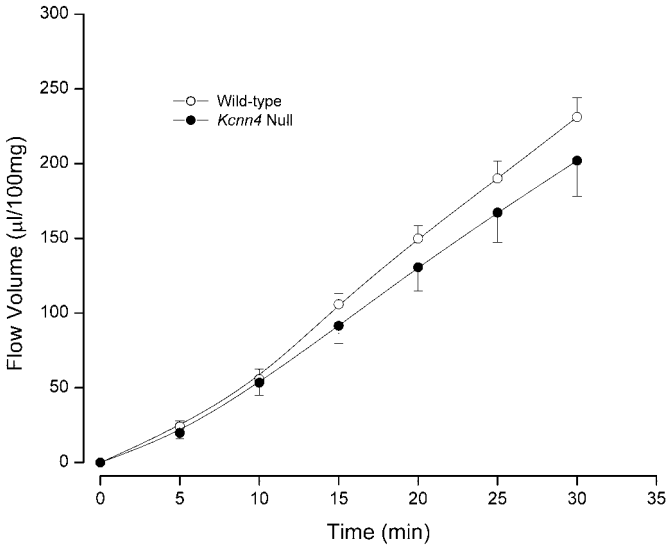

FIG. 5. **Saliva flow from wild-type and *Kcnn4* null mice.** Flow volume was measured at the indicated time points stimulated by pilocarpine (1 mg/kg body weight). Flow volume from the parotid glands of wild-type (○, $n = 12$) and *Kcnn4* null mice (●, $n = 12$) is depicted. Mean values with S.E. limits are shown.

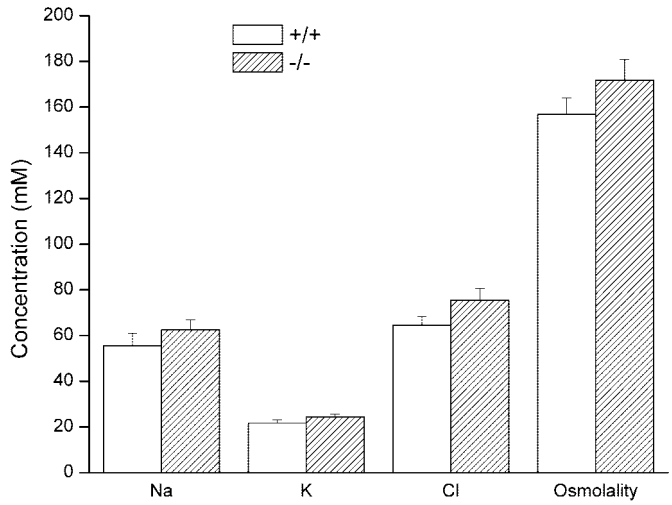

FIG. 6. **Saliva contents from wild-type and *Kcnn4* null mice.** The concentration of the indicated substance secreted upon stimulation with 1 mg/kg body weight pilocarpine. Shown are data from the parotid glands of wild-type (+/+, $n = 12$) and *Kcnn4* null (−/−, $n = 12$) animals as indicated. Mean values with S.E. limits are depicted.

gous males and females do not differ from their wild-type littermates (mean ± S.E. values are as follows: male +/+, 27.0 ± 1.1 g with $n = 36$; male −/−, 27.3 ± 1.0 g with $n = 42$; female +/+, 21.5 ± 0.5 g with $n = 40$; female −/−, 22.9 ± 0.6 g with $n = 36$). In contrast, the weight of the parotid glands from homozygote null male mice was significantly higher than that from wild-type male animals (+/+, 29.2 ± 1.2 mg with $n = 36$; and −/−, 32.8 ± 1.2 mg with $n = 42$; $p = 0.04$). A similar trend was observed in females but did not achieve statistical significance (+/+, 26.4 ± 0.9 mg with $n = 40$; −/−, 28.0 ± 0.9 mg with $n = 36$; $p = 0.25$). Histological examination of major organ systems did not reveal any gross differences between wild-type and knock-out tissues.

IK1 Channels and T lymphocyte Physiology—Ca^{2+}-mobilizing agents induce shrinkage of CD4+ T lymphocytes, which can be specifically blocked by clotrimazole (16). The Northern blot in Fig. 2*A* shows the expression of IK1 mRNA in CD4+ lymphocytes from wild-type mice (+/+). This band is absent in *Kcnn4* null animals (−/−). *Panel B* of Fig. 2 shows that the Ca^{2+} ionophore, ionomycin (5 µM), induced T lymphocytes isolated from wild-type mice (Fig. 2*B*, ■) to shrink nearly 20% ($n = 6$). In contrast, the ionomycin-induced shrinkage of lymphocytes from *Kcnn4* null (Fig. 2*B*, ○) animals was dramatically reduced ($n = 6$). Similarly, the IK1-specific channel blocker clotrimazole (10 µM) essentially eliminated the cell shrinkage in wild-type CD4+ lymphocytes (data not shown).

IK1 Channels and Red Blood Cell Physiology—As described above, red blood cells have a Ca^{2+}-activated conductive K^+ permeability believed to be mediated by the Gardos channel (7). The data in Fig. 3*A* show that this permeability is indeed encoded by the *Kcnn4* gene. The large A23187-stimulated, clotrimazole-sensitive ^{86}Rb influx into red blood cells from wild-type animals was nearly eliminated in the *Kcnn4* (−/−) erythrocytes.

We also examined the ability of the IK1/Kcnn4 Gardos channel to control red blood cell volume by measuring the effect of A23187 on osmotic fragility for red cells. Fig. 3*B* shows the percentage of red cell lysis from wild-type animals at the indicated relative solution tonicity in the absence (○) and presence (■) of 5 µM A23187, which was used to increase intracellular Ca^{2+} levels. As shown previously (11, 27), activation of the K^+ permeability (with consequent cell shrinkage) protects cells from hypotonic lysis. In the absence of A23187, 50% of the cells lysed when relative tonicity was reduced to 0.47. Activation of Ca^{2+}-gated potassium channels lowered to 0.28 the relative tonicity at which 50% of the cells lysed. In contrast, the relative tonicity at which red cells from *Kcnn4* null animals showed 50% lysis was not reduced by A23187 but even showed a slight increase (Fig. 3*C*).

IK1 Channels and Parotid Physiology—As described above, parotid acinar cells express two types of Ca^{2+}-activated potassium channels (6). One type has little time or voltage dependence and is blocked by clotrimazole. The second type has strong voltage and time dependence and is blocked by paxilline. Examples of these currents from a parotid acinar cell patched with a pipette solution containing 250 nM free Ca^{2+} are illustrated in Fig. 4*B*. Shown in the *inset* are raw currents from 40-msec pulses to −110, −30, +10, and +50 mV from a holding potential of −70 mV. There are time-independent currents apparent at all potentials; an additional time-dependent current component was activated over the 40-msec duration of large depolarizing pulses. The main part of Fig. 4*B* shows the magnitude of the current measured at the end of the voltage pulses. This current is composed of linear (Fig. 4*B*, *dashed line*) and highly non-linear components. These currents are K^+-selective as evidenced by the negative zero current potential. The linear component is preferentially blocked by clotrimazole (not shown; see Ref. 6).

We have suggested previously that the time- and voltage-independent component of the parotid Ca^{2+}-activated K^+ current is due to expression of the *Kcnn4* gene (6). The data in Fig. 4*A* support this hypothesis. The Northern blot shows expression of IK1 mRNA in the parotid gland from wild-type mice (+/+). This band is absent in *Kcnn4* null animals (−/−) and is of a reduced intensity in mice heterozygous for the null mutation (+/−).

If the time- and voltage-independent component of the Ca^{2+}-activated K^+ current seen in Fig. 4*B* is, in fact, due to the expression of *Kcnn4*, then this component should disappear in the *Kcnn4* null animals. *Panel C* of Fig. 4 shows that this was indeed the case. The *inset* of Fig. 4*C* illustrates whole-cell currents from a parotid acinar cell isolated from a *Kcnn4* null mouse measured under conditions identical to those described for *panel B*. The main part of Fig. 4*C* shows the voltage-dependence of currents measured at the end of the 40-msec

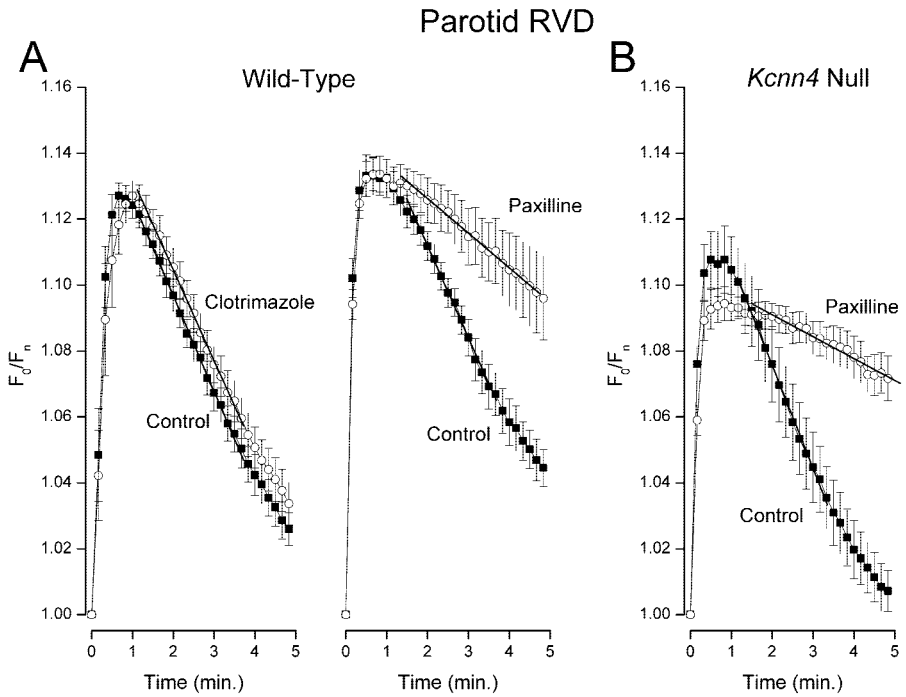

FIG. 7. **Parotid cell regulatory volume RVD in wild-type and *Kcnn4* null animals.** *A*, time dependence RVD in parotid acinar cells from wild-type animals. Relative fluorescence was used as a measure of cell volume in response to a 30% reduction in bathing fluid tonicity at time zero. *Left*, RVD in the absence (■, $n = 7$) and presence (○, $n = 7$) of 1 μM clotrimazole. *Right*, RVD in the absence (■, $n = 6$) and presence (○, $n = 6$) of 1 μM paxilline. *B*, RVD of cells from *Kcnn4* null animals in the absence (■, $n = 6$) and presence (○, $n = 6$) of 1 μM paxilline. *Symbols* represent mean values with S.E. limits. The *thin lines* in all graphs serve only to connect the symbols. The *thick lines* in each graph are least squares fits to the early linear phase of RVD with the following rates: wild-type, 4.8×10^{-4} sec^{-1} (control) and 4.6×10^{-4} sec^{-1} (clotrimazole); wild-type, 4.7×10^{-4} sec^{-1} (control) and 1.75×10^{-4} sec^{-1} (paxilline); and *Kcnn1* null, 5.2×10^{-4} sec^{-1} (control) and 1.1×10^{-4} sec^{-1} (paxilline).

pulses just as in Fig. 4*B*. The time- and voltage-independent currents apparent in the cell from the wild-type animal in Fig. 4*B* are totally absent in the current data from the *Kcnn4* null mouse.

To obtain a quantitative assessment of IK1 channel currents in wild-type and *Kcnn4* null mice, we measured the current just after the step to −110 mV. We also measured cell capacitance to normalize measured currents for cell size. Mean current density (at −110 mV) in cells from wild-type animals was -55 ± 17 pA/pF ($n = 7$), and it was -2.7 ± 1 pA/pF ($n = 11$) in cells from *Kcnn4* null mice. With an average cell capacitance of 11 pF, this latter value is equivalent to a resistance of ~3.8 gigaohms. Because this value is near the expectation for normal patch clamp seal resistance, a reasonable conclusion is that essentially all of the parotid acinar cell, time- and voltage-independent Ca^{2+}-activated K^+ current was eliminated in the *Kcnn4* null mice.

A comparison of the magnitude of the time- and voltage-dependent currents in Fig. 4 suggests an increase in this component in the *Kcnn4* null animal, as if in compensation for the loss of the IK1 channels. A definitive assessment of this issue at this time is difficult, as we have consistently observed an apparently concomitant decrease in the magnitude of the time-dependent current as the time-independent current activates after achieving the whole-cell configuration of the patch clamp technique. This issue is currently under active investigation; however, in the interim, we have compared these two current components (at 50 mV) by recording the time-dependent current (at 40 msec) in cells from wild-type animals just after achieving whole-cell mode and prior to significant development of the IK1 component. The current was 170 ± 12 pA ($n = 6$) in wild-type cells and 310 ± 130 pA/pF ($n = 11$) in cells from *Kcnn4* null animals, a significant difference ($p = 0.02$). Thus, either some compensation occurred in the *Kcnn4* null animals or the complexity of the interaction between the two types of channels clouds this assessment. Our ongoing investigation is aimed at clarifying this issue.

To test the role of IK1 in salivary fluid secretion *in vivo*, we measured saliva flow in cannulated parotid ducts. The pooled results from several such experiments are illustrated in Fig. 5. Pilocarpine-stimulated saliva volume from wild-type (Fig. 5, ○) and *Kcnn4* null (●) mice was measured over a 30 min period. Clearly, ablating the expression of IK1 channels produced little or no change in saliva flow.

We also investigated the composition of the saliva produced by stimulation with pilocarpine. There was little or no difference in sodium, potassium, and chloride content of saliva between wild-type and *Kcnn4* null mice as illustrated in Fig. 6. Also, as illustrated in the figure, there was little or no difference in the saliva osmolality. We also measured the amount of protein secreted in the saliva. We found 2.67 ± 0.38 μg/ml protein in saliva from wild-type animals and 2.71 ± 0.32 μg/ml in saliva from *Kcnn4* null mice. Although the measured level of all saliva constituents increased slightly in the *Kcnn4* null mice, none of these differences was statistically significant.

Many cells, including those in parotid glands, can dynamically alter their volume in response to changes in bathing solution osmolarity. Regulatory volume decrease (RVD) is a regulated reduction in cell volume in response to the rapid cell swelling produced by a sudden reduction in extracellular solution osmolarity. We show, in Fig. 7, the RVD of parotid acinar cells in response to a 30% reduction in solution osmolarity. In wild-type animals (Fig. 7*A*) blocking IK1 channels with clotrimazole (1 μM) had a negligible effect on RVD, but blocking maxi-potassium channels with paxilline (1 μM) reduced the RVD rate by a factor of 2.7. These results suggest little or no role for IK1 channels in RVD in parotid acinar cells. This assumption was confirmed by measurements of RVD in *Kcnn4* null mice (Fig. 7*B*); the control RVD rate of the *Kcnn4* null mice was very similar to the rate in wild-type mice. If IK1 channels

contributed significantly to the RVD process, the RVD rate would be decreased in the *Kcnn4* null mice. Not only was the rate not reduced, it was actually ~10% faster in cells from the *Kcnn4* null mice. Such an increase in RVD rate could be the result of an enhancement of some other K^+ efflux pathway in the *Kcnn4* null animals. The small blunting of the magnitude of the initial volume increase compared with that in wild-type animals is consistent with this idea, as is the stronger effect of paxilline seen in the *Kcnn4* mice. In these animals, paxilline decreased the RVD rate by a factor of 4.7 compared with the 2.7-fold effect seen in wild-type animals.

DISCUSSION

The presence in red cells of a latent K^+ permeability activated by the elevation of intracellular [Ca^{2+}] was first described in 1958 (7) and was shown to represent Ca^{2+}-activated K^+ channel activity of intermediate conductance. Pharmacological studies with charybdotoxin, maurotoxin, clotrimazole, and small molecule inhibitors of related structure have suggested that the entire Ca^{2+}-activated K^+ conductance of the red cell is mediated by IK1/Kcnn4 channels. However, Kcnn1/SK1 mRNA has been detected by reverse transcription PCR in murine erythroid precursor cells (28) and in human reticulocytes (29). The current data provide confirmation that the *Kcnn4* gene is responsible for essentially all Ca^{2+}-activated K^+ permeability in the mature circulating erythrocyte of the mouse. This is shown by the near abolition of A23187-stimulated ^{86}Rb influx and by the absence of A23187-induced resistance to hypo-osmotic lysis in *Kcnn4* null red cells. Additional preliminary data (not shown) indicate the abolition of A23187-induced shrinkage of red cells from *Kcnn4* null animals as determined by light scattering measurements and the near abolition of K^+ channel activity as measured by on-cell and nystatin-perforated whole-cell patch clamp recordings.

IK1 activity is elevated in red cells from sickle disease patients and in red cells from mouse models of sickle disease (10). IK1-mediated solute and water loss from red cells is further exacerbated by the elevated circulating levels of inflammatory mediators that activate erythroid IK1. Thus, the *Kcnn4* null mouse should present an opportunity to test the role of IK1 as a risk modifier in mouse models of sickle disease. It also provides an opportunity to test the specificity of IK1 blockers, which are under development for the pharmacological treatment of sickle disease (12).

The sensitivity of the Ca^{2+}-induced shrinkage in CD4+ T lymphocytes to clotrimazole suggests the involvement of IK1 in this response (16). The near elimination of the ionomycin-induced cell shrinkage in *Kcnn4* null animals confirms that the Ca^{2+}-activated K^+ channels in these cells are indeed the result of the expression of this gene and are critical for such active volume changes.

Our results also show that *Kcnn4* encodes the time- and voltage-independent, intermediate conductance, Ca^{2+}-activated K^+ channel in parotid acinar cells. As noted in the Introduction, previous studies suggested that IK rather than BK channel activity would underlie secretion from salivary glands, consistent with the robust expression of IK1 mRNA in these glands (6). It was, therefore, surprising to find little or no change in the parotid gland fluid secretion rate between wild-type and *Kcnn4* null animals stimulated with pilocarpine (Fig. 5*A*). There was also very little change in the composition of saliva or in RVD (Figs. 6 and 7). The electrophysiological data (Fig. 4 and associated text) and the increased sensitivity of RVD to the BK channel inhibitor paxilline (Fig. 7) suggested an increased BK channel activity in the *Kcnn4* null mice. Such an increase in BK channel activity could compensate for the loss of IK channels in the *Kcnn4* null mice and so preserve fluid secretion. However, the observed reduction in maxi-potassium current upon IK1 channel activation in wild-type animals complicates the efforts to produce a reliable, quantitative estimate of any change in maxi-potassium expression in *Kcnn4* null animals. As noted earlier, this important issue is currently the focus of investigation. The investigation of salivary gland fluid secretion in mice without BK channels (30) will provide further insight into the possibility of the interdependence of BK and IK channel activity in parotid acinar cells.

Acknowledgments—We thank Lin-Chie Pong, Jill Thompson, Mark Wagner, Pam McPherson, Laurie Koek, and Jennifer Scantlin for technical assistance and Alicia Rivera and David H. Vandorpe for helpful discussions. We also thank Peter Keng and Deborah Fowell for assistance in the T lymphocyte experiments and Greg Boivin for histological analysis.

REFERENCES

1. Joiner, W. J., Wang, L., Tang, M. D., and Kaczmarek, L. K. (1997) *Proc. Natl. Acad. Sci. U. S. A.* **94,** 11013–11018
2. Ishii, T. M., Silvia, C., Hirschberg, B., Bond, C. T., Adelman, J. P., and Maylie, J. (1997) *Proc. Natl. Acad. Sci. U. S. A.* **94,** 11651–11656
3. Logsdon, N. J., Kang, J., Togo, J. A., Christian, E. P., and Aiyar, J. (1997) *J. Biol. Chem.* **272,** 32723–32726
4. Vandorpe, D. H., Shmukler, B. E., Jiang, L., Lim, B., Maylie, J., Adelman, J. P., de Franceschi, L., Cappellini, M. D., Brugnara, C., and Alper, S. L. (1998) *J. Biol. Chem.* **273,** 21542–21553
5. Warth, R., Hamm, K., Bleich, M., Kunzelmann, K., von Hahn, T., Schreiber, R., Ullrich, E., Mengel, M., Trautmann, N., Kindle, P., Schwab, A., and Greger, R. (1999) *Pflugers Arch.* **438,** 437–444
6. Nehrke, K., Quinn, C. C., and Begenisich, T. (2003) *Am. J. Physiol.* **284,** C535–C546
7. Gardos, G. (1958) *Biochim. Biophys. Acta* **30,** 653–654
8. Hoffman, J. F., Joiner, W., Nehrke, K., Potapova, O., Foye, K., and Wickrema, A. (2003) *Proc. Natl. Acad. Sci. U. S. A.* **100,** 7366–7371
9. Brugnara, C., Gee, B., Armsby, C. C., Kurth, S., Sakamoto, M., Rifai, N., Alper, S. L., and Platt, O. S. (1996) *J. Clin. Investig.* **97,** 1227–1234
10. Brugnara, C., De Franceschi, L., Bennekou, P., Alper, S. L., and Christophersen, P. (2001) *Drug News Perspect.* **14,** 208–220
11. De Franceschi, L., Saadane, N., Trudel, M., Alper, S. L., Brugnara, C., and Beuzard, Y. (1994) *J. Clin. Investig.* **93,** 1670–1676
12. Stocker, J. W., De Franceschi, L., McNaughton-Smith, G. A., Corrocher, R., Beuzard, Y., and Brugnara, C. (2003) *Blood* **101,** 2412–2418
13. Ghanshani, S., Wulff, H., Miller, M. J., Rohm, H., Neben, A., Gutman, G. A., Cahalan, M. D., and Chandy, K. G. (2000) *J. Biol. Chem.* **275,** 37137–37149
14. Fanger, C. M., Rauer, H., Neben, A. L., Miller, M. J., Wulff, H., Rosa, J. C., Ganellin, C. R., Chandy, K. G., and Cahalan, M. D. (2001) *J. Biol. Chem.* **276,** 12249–12256
15. Wulff, H., Beeton, C., and Chandy, K. G. (2003) *Curr. Opin. Drug Discovery Devel.* **6,** 640–647
16. Elliott, J. I., and Higgins, C. F. (2003) *EMBO Rep.* **4,** 189–194
17. Hayashi, T., Young, J. A., and Cook, D. I. (1996) *J. Membr. Biol.* **151,** 19–27
18. Maruyama, Y., Nishiyama, A., and Teshima, T. (1986) *Jpn. J. Physiol.* **36,** 219–223
19. Wegman, E. A., Ishikawa, T., Young, J. A., and Cook, D. I. (1992) *Am. J. Physiol.* **263,** G786–G794
20. Ishikawa, T., Murakami, M., and Seo, Y. (1994) *Pflugers Arch.* **428,** 516–525
21. Park, K., Case, R. M., and Brown, P. D. (2001) *Arch. Oral Biol.* **46,** 801–810
22. Takahata, T., Hayashi, M., and Ishikawa, T. (2003) *Am. J. Physiol.* **284,** C127–C144
23. Hayashi, T., Poronnik, P., Young, J. A., and Cook, D. I. (1996) *J. Membr. Biol.* **152,** 253–259
24. Krane, C. M., Melvin, J. E., Nguyen, H. V., Richardson, L., Towne, J. E., Doetschman, T., and Menon, A. G. (2001) *J. Biol. Chem.* **276,** 23413–23420
25. Bers, D., Patton, C., and Nuccitelli, R. (1994) *Methods Cell Biol.* **40,** 3–29
26. Rivera, A., Rotter, M. A., and Brugnara, C. (1999) *Am. J. Physiol.* **277,** C746–754
27. Halperin, J. A., Brugnara, C., and Nicholson-Weller, A. (1989) *J. Clin. Investig.* **83,** 1466–1471
28. Schmukler, B., Bond, C., Wilhelm, S., Bruening-Wright, A., Maylie, J., Adelman, J. P., and Alper, S. L. (2001) *Biochim. Biophys. Acta* **1518,** 36–46
29. Zhang, B., Kohli, V., Adachi, R., Lopez, J., Udden, M., and Sulivan, R. (2001) *Biochemistry* **40,** 3189–3195
30. Meredith, A. L., Thorneloe, K. S., Werner, M. E., Nelson, M. T., and Aldrich, R. W. *J. Biol. Chem.* **279,** 36746–36752

Physiological Roles of the Intermediate Conductance, Ca^{2}+-activated Potassium Channel Kcnn4

Ted Begenisich, Tesuji Nakamoto, Catherine E. Ovitt, Keith Nehrke, Carlo Brugnara, Seth L. Alper and James E. Melvin

J. Biol. Chem. 2004, 279:47681-47687.
doi: 10.1074/jbc.M409627200 originally published online September 3, 2004

THE JOURNAL OF BIOLOGICAL CHEMISTRY
Vol. 280, No. 8, Issue of February 25, pp. 7407–7408, 2005

Printed in U.S.A.

Additions and Corrections

Vol. 272 (1997) 11908–11915

Convenient isolation and kinetic mechanism of glutathionylspermidine synthetase from *Crithidia fasciculata.**

Kerstin Koenig, Ulrich Menge, Michael Kiess, Victor Wray, and Leopold Flohé

Since the discovery of trypanothione (N^1,N^8-bis(glutathionyl)-spermidine), it has been debated whether its biosynthesis in *Crithidia fasciculata* requires one or two enzymes. After two related genes implicated in trypanothione synthesis had become available, the correct assignment of sequence to function remained controversial because heterologous expression did not yield active proteins (Tetaud, E., Manai, F., Barrett, M. P., Nadeau, K., Walsh, K. T., and Fairlamb, A. H. (1998) *J. Biol. Chem.* **273,** 19383–19390). In 2002, however, Oza *et al.* (Oza, S. L., Ariyanayagam, M. R., and Fairlamb, A. H. (2002) *Biochem. J.* **364,** 679–686) reported the functional expression of a *gsps* DNA sequence of *C. fasciculata* (GenBank™ accession number U66520.2) that did not comply with the partial amino acid sequences of glutathionylspermidine synthetase (GspS), as published in our above article.

A deep-frozen sample of the GspS preparation that had been isolated from *C. fasciculata* and functionally characterized by us was therefore reinvestigated. It still displayed GspS activity and no trypanothione synthetase (TryS) activity, as originally stated. Matrix-assisted laser desorption ionization time-of-flight analysis of a tryptic digest, however, did not reveal the presence of any of the peptide sequences previously reported but instead revealed many mass peaks complying with the GspS sequence. Coverage was 45% of the deduced GspS sequence and 70% of theoretically detectable peptide masses. Major mass signals that could not be attributed to the GspS sequence were absent. Therefore, the sequence assignment to GspS by Oza *et al.* is the correct one.

The partial sequences previously reported by us are contained in the expression product of *trys* (GenBank™ accession number AY603101), the homologous trypanothione synthetase that catalyzes both steps of trypanothione biosynthesis (Comini, M. A., Menge, U., Wissing, J., and Flohé, L. (2005) *J. Biol. Chem.* **280,** 6850–6860). Thus *C. fasciculata* is equipped with two enzymes, one catalyzing the formation of glutathionylspermidine only and the other one being competent to catalyze both steps of the trypanothione synthesis.

How the wrong assignment of partial TryS sequences to GspS occurred could no longer be assessed with certainty. According to our laboratory notes, peptide sequencing was not performed with the same batch that had been functionally characterized. The sequenced sample had been purified to electrophoretic homogeneity by means of the chromatographic scheme described for the isolation of GspS but had not been subjected to the initial liquid/liquid extraction that separates and denatures most of the TryS. This may explain how ultimately an inactive TryS protein was obtained and sequenced instead of the presumed GspS. Leopold Flohé, who supervised this work, takes the full and sole responsibility for the erroneous interpretation of the sequence information.

*Amended by Marcelo Comini, Ulrich Menge, and Leopold Flohé.

Vol. 279 (2004) 47681–47687

Physiological roles of the intermediate conductance, Ca^{2+}-activated potassium channel Kcnn4.

Ted Begenisich, Tesuji Nakamoto, Catherine E. Ovitt, Keith Nehrke, Carlo Brugnara, Seth L. Alper, and James E. Melvin

Page 47684, Fig. 4A: There was an error in the labeling *above* the *lanes* in *panel A*. The correct figure is shown below.

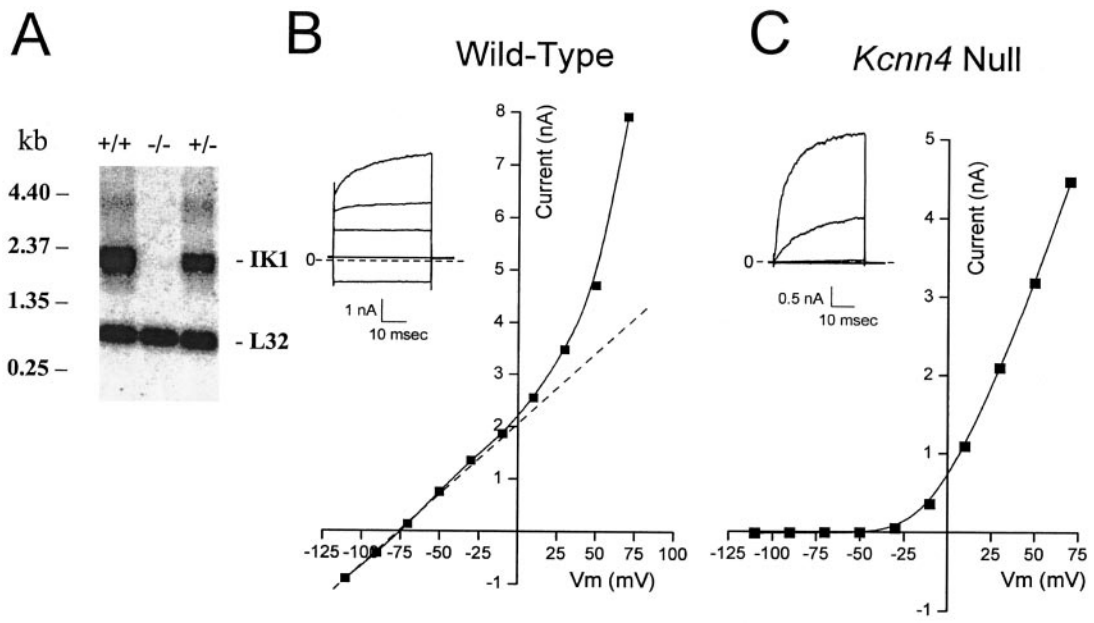

FIG. 4